

Graphical Representations of Experimental and ANN Predicted Data for Mechanical and Electrical Properties of AlSiC Composite Prepared by Stir Casting Method

Philip O. Babalola^{1*}, Christian A. Bolu¹, Anthony O. Inegbenebor¹, Oluseun Kilanko¹

Department of Mechanical Engineering, College of Engineering, Covenant University, Ota, Nigeria
E-mail address: phillip.babalola@covenantuniversity.edu.ng

Abstract. Artificial Neural network is a field of man-made intelligence that is able to undertake design prediction, mechanical property forecast, and process selection. In this paper, Aluminium Silicon Carbide composite was developed by reinforcing aluminium metal with silicon carbide powder using stir casting method. The produced aluminium matrix composites (AMC) were subjected to tensile, hardness and electrical tests to obtain tensile extension (mm), load (N), modulus (N/mm²), yield strength (MPa), hardness (HV), ultimate tensile strength (MPa), tenacity at fracture (gf/tex), time at fracture (s), hardness (HV), conductivity (M Ω /m), and tensile stress (MPa) data. Artificial Neural Network (ANN) was then used to train, test, and validate the obtained experimental data and then predict new set of data. The experimental and ANN predicted data were represented using graphical illustrations. The results showed that ANN could be used to replace rigorous, costly and time consuming experimental exercise with minimal loss in accuracy.

Keywords: AlSiC composite, artificial neural network (ANN), mechanical properties, electrical properties, stir casting

1. Introduction

Aluminium metal is the most severely used non-ferrous metal in our world today and it is only second to steel, when it comes to automobile body frame [1], with 5xxx and 6xxx series on the lead. Light weight, high strength, and high resistance to corrosion in an aggressive environment make aluminium a suitable material for use in conventional and non-conventional applications. Aluminium also responds readily to strengthening mechanisms. However, aluminium does not perform very well in high temperature applications due to its low melting temperature. It also has very little resistance to abrasive wear because of small hardness value [2]. Improved mechanical properties is obtained by reinforcing aluminium alloy matrix with ceramic materials [3-6]. Some ceramic materials like alumina, B₄C, SiC, Si₃N₄, AlN, TiC, TiB₂, TiO₂ and hard metals such as tungsten and titanium are used for this purpose [7]. The resultant aluminium matrix composites now have numerous use in reciprocating internal combustion engine members (cylinder liners, pistons, pushrods, cylinder blocks), rotors brake for high speed locomotives, transmission parts, turbocharger vanes, forks for gear shift, clutch plate, golf clubs, bicycles, electronic boards, and heat fins. Bringing aluminium and reinforcing material together may be done using processing methods such as powder metallurgy, cryomilling, vacuum infiltration, vacuum hot pressing, thixoforming, co-spray deposition process, compocasting, squeeze casting, centrifugal casting, laser alloying and stir casting methods [6, 8]. Stir casting method is used in this work due to its cost-effectiveness and ease of varying and monitoring of processing parameters. Many studies have been conducted on properties and characterization of Al/SiCp composites [9-13]. Evaluated properties of the composites depend on the particularly critical one for the material application. Some of these properties are tensile, hardness, thermal conductivity, electrical conductivity, fatigue, creep, wear rate and so on.

However, the same properties are now being predicted using Artificial Neural Network (ANN) method. Kavimani and Prakash used ANN and Taguchi method to predict wear rate properties of magnesium composite [14], while Rashed and Mahmoud in their work used ANN to predict the same property but



with aluminium composite [15]. Apart from material properties, ANN is also used in process parameters in surface engineering [16], machining [17] and composite.

2. Materials and Methods

In this work, stir casting method was adopted to synthesize samples of AMCs using 1170Al reinforced with Silicon Carbide (SiC) particulates of 3 μm , 9 μm , 29 μm , and 45 μm sizes respectively. The chemical composition of Aluminium and Silicon Carbide are presented in Table 1 and Table 2 below.

Table 1 The Compositions in Percentage of Aluminium Ingot Used in the Experiment

Fe	Mg	Sn	Cu	Zn	Ti	Si	Pb	Mn	Al
0.232	0.0027	0.007	0.0006	0.0016	0.006	0.078	0.0012	0.000	99.66

Table 2 The Chemical Composition in Percentage of Silicon Carbide

Si	Al	Fe	C	SiO ₂	Magnetic Iron	SiC
0.80	0.30	0.20	0.50	0.60	0.04	97.6

The liquid metallurgy method (stir casting technique) was used to formulate AMC. An oil-fired tilting furnace was used to melt measured mass of 1170Al to 750 °C inside a graphite crucible. A K-type thermocouple was used to monitor the temperature of the melt to avoid overheating and energy wastage. A mould preheated to 450 °C was used to receive the melt where it was mixed with the help of an impeller to form a fine vortex. SiC particles heated to temperature of 1100 °C was then introduced into the melt simultaneously with mechanical stirring at 500rpm for about 5mins. Mixing occurs when the slurry is at semisolid form.

The melt behaves as a solid when no stress is involved but flows like a liquid when pressure is applied- this is thixotropic property. Uniform dispersion is produced by introducing particles when cooling of the melt is combined with rigorous agitation. The agitation helped in breaking the liquid-solid mixture by break down the dendritic structure. The AMCs having different particle sizes (3 μm , 9 μm , 29 μm and 45 μm) and each size with different weight percentage (2.5, 5.0, 7.5 and 10 wt %) of SiC were fabricated by the same procedure.

2.1 Tensile test

All specimens produced through stir casting method had circular cross-section with dimensions of 110 mm Φ and 30 mm length. Five tensile specimen with dimensions of 5 mm \times 10 mm with a gauge length of 25 mm were machined out and tested in Universal Testing Machine (Instron: Model 3369) of 30kN load using ASTM International E8/E8M-09 standard. Five measurements (modulus) were recorded for each sample and the average was calculated.

2.2 Microhardness test

Microhardness measurements were carried according to ASTM Standard E 384. Test machine was LECO 700AT with a load of 492.3 mN and a dwell time of 10 s. Surface preparation was done with emery papers down to 1000 mesh. Six tests were conducted for each sample and the average recorded.

2.3 Electrical conductivity

Specimen of each cast were cut out and milled in the machine shop for electrical conductivity testing. The working voltage of 20 mV was selected in 4-point probe machine on samples with dimensions 10 mm L \times 10 mm B \times 100 mm H. Keithley Instruments Model 2400 was used to generate current, voltage, conductivity and resistivity for each sample.

2.4 ANN predicted data

ANN was used for modelling and forecasting tensile, electrical conductivity and micro-hardness properties. ANN architecture as shown in Figure 1 was employed to train, test and validate the measured data and then generate new forecasted data. Figure 1 consists of number of joints, arranged in layers that are identified as output layer, hidden layer, and input layer. Iterative computations are done viz-a-viz input layers through network structure depicted by the hidden layers until it arrives at the output layers. The input is a 3x17 matrix, representing 17 samples of 3 elements (see Table 3). Three input elements are percentage weight of aluminium, percentage weight of SiC and size of SiC particle. The output (target) is a 11x17 matrix, representing 17 samples of 11 elements (see Table 4). The eleven output elements are microhardness, yield strength, tensile extension, modulus, ultimate tensile strength, tensile stress, time at fracture (break), load at maximum extension, tenacity, electrical resistivity and conductivity. Training and simulation steps used exactly 70% of the data, validation steps used 15% of the data, while remaining 15% was used for testing the network. The architecture of the network can be represented as (3, HL, 11), where HL is the hidden layer, hence the network topology (3,15,11), used the trained data to understand the weights, and records the Mean Square Error (MSE) values.

A dataset of experimental results was grouped into three categories: testing, training, and validation of the artificial neural network. The weights of all the connecting nodes is adjusted during training sessions until error level no longer improved. Coefficient of determination B (also called R^2 coefficient) used to measure the effectiveness of ANN is denoted by:

$$B = 1 - \frac{\sum_{i=1}^M (O(p^{(i)}) - o^{(i)})^2}{\sum_{i=1}^M (O^{(i)} - o)^2} \quad (1)$$

where $O(p(i))$ is the i th forecasted property characteristic, $O(i)$ is the i th experimental value, O is the mean value of $O(i)$, and M is the number of test data. Good output approximation competencies of ANN is measured with higher B coefficients. Hence, best quality could be deduced when B is equal or greater than 0.9. The relationship between outputs and targets is measured by the regression R values. A close relationship is known by an R value of 1, while 0 denotes random relationship and from Figure 2, training has R value of 1.0, validation has R value of 0.96298, test has R value of 0.90984 and all has R value of 0.96361. It can be inferred that there is close relationship between the outputs and the targets. **Training** data were used to modify the network during training using its error, **validation** samples were used to measure network generalization and to halt training when generation no longer improve, while **testing** data have no direct effect on training and so provided an autonomous measurement of network evaluation during and after training (Figure 2 and Figure 3). The summary of ANN results, a pattern recognizing tool is indicated in Figure 4.

Table 3 ANN Input Data

S/N	Al %wt.	SiC %wt.	SiC Size (μm)	
1	100	0		0
2	97.5	2.5		3 x 10 ⁻⁶
3	95	5	3 x 10 ⁻⁶	
4	92.5	7.5	3 x 10 ⁻⁶	
5	90	10	3 x 10 ⁻⁶	
6	97.5	2.5		9 x 10 ⁻⁶
7	95	5	9 x 10 ⁻⁶	
8	92.5	7.5	9 x 10 ⁻⁶	
9	90	10	9 x 10 ⁻⁶	
10	97.5	2.5		2.9 x 10 ⁻⁵
11	95	5	2.9 x 10 ⁻⁵	
12	92.5	7.5	2.9 x 10 ⁻⁵	
13	90	10	2.9 x 10 ⁻⁵	
14	97.5	2.5		4.5 x 10 ⁻⁵

15	95	5	4.5 x 10 ⁻⁵
16	92.5	7.5	4.5 x 10 ⁻⁵
17	90	10	4.5 x 10 ⁻⁵

Table 4 ANN Output (Target) Data

S/N	Extension at Maximum Tensile Extension (mm)	Load at Maximum Tensile Extension (N)	Modulus (N/mm ²)	Yield Strength (MPa)	Ultimate Tensile Strength (MPa)	Tenacity at Fracture (gf/tex)	Time at Fracture (Standard) (sec)	Hardness (HV)	Conductivity, (M Ω /m)	Resistivity, ($\mu\Omega$ -m)	Tensile Stress at Maximum Tensile Extension (MPa)
1	20.783118	720.0062	402.413324	40.8	61.3	845.6629	40.8032	19.6	70.25378	0.014234	15.175522
2	10.685998	353.2760581	1293.428876	29.6	37.2	381.4674	21.3124	20.05	68.82136	0.01453	8.160014
3	10.84656	419.3332365	1028.56321	35	53	438.4278	21.65	23.6	67.70123	0.014771	9.35811
4	7.945935	314.260534	1517.59211	24.25	31.625	320.9439	15.883	24.75	64.14723	0.015589	6.76695
5	8.6769125	420.843328	878.9286575	22.25	28.25	434.3051	17.3	25.9	48.74027	0.020517	5.649625
6	8.143038	688.626658	1290.11912	30.4	40	711.5514	16.22	22.95	67.83901	0.014741	13.039944
7	7.15681496	374.451228	888.772108	16.8	24	383.5274	14.3	24.65	62.96254	0.015882	6.403696
8	7.01875	498.46985	1092.8752	21.625	26.5	519.2085	13.975	26.05	59.82686	0.016715	10.044365
9	6.4023433	291.1302844	760.3567167	11.667	13.867	301.7488	12.73333	26.2	48.96254	0.020424	4.4393267
10	11.061328	698.093155	1233.86522	30.75	41.625	721.5803	22.075	23.55	68.63504	0.01457	13.083903
11	9.46796	688.299396	969.405182	36	47.6	746.2332	18.7772	25.2	66.96015	0.014934	14.489662
12	6.3033333	62.090076	1326.21316	31.667	39.667	63.55679	12.57733	33.65	65.26178	0.015323	1.14747
13	13.491654	615.047286	990.415216	28	42.1	756.6384	46.5948	34.25	56.63504	0.017657	12.173872
14	12.404812	503.2448	580.916218	22.8	33.46	610.1167	14.2568	23.85	67.80000	0.014749	8.624638
15	12.6141	453.2824975	793.2229175	34.5	44.75	497.3207	15.1	33.45	61.58468	0.016238	9.3490325
16	6.7462164	762.192954	935.028496	19.8	27.62	780.5672	40.42	33.65	63.45271	0.01576	13.021274
17	10.785468	382.0129175	645.46291	29.125	39.625	398.2237	21.52	35.2	50.27102	0.019892	6.3503725

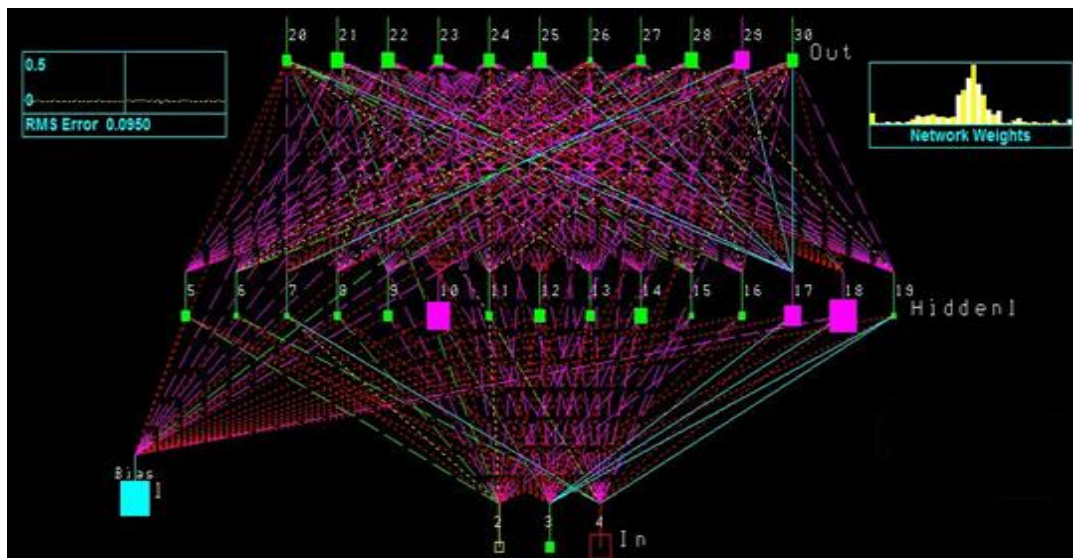


Fig. 1 ANN Architecture

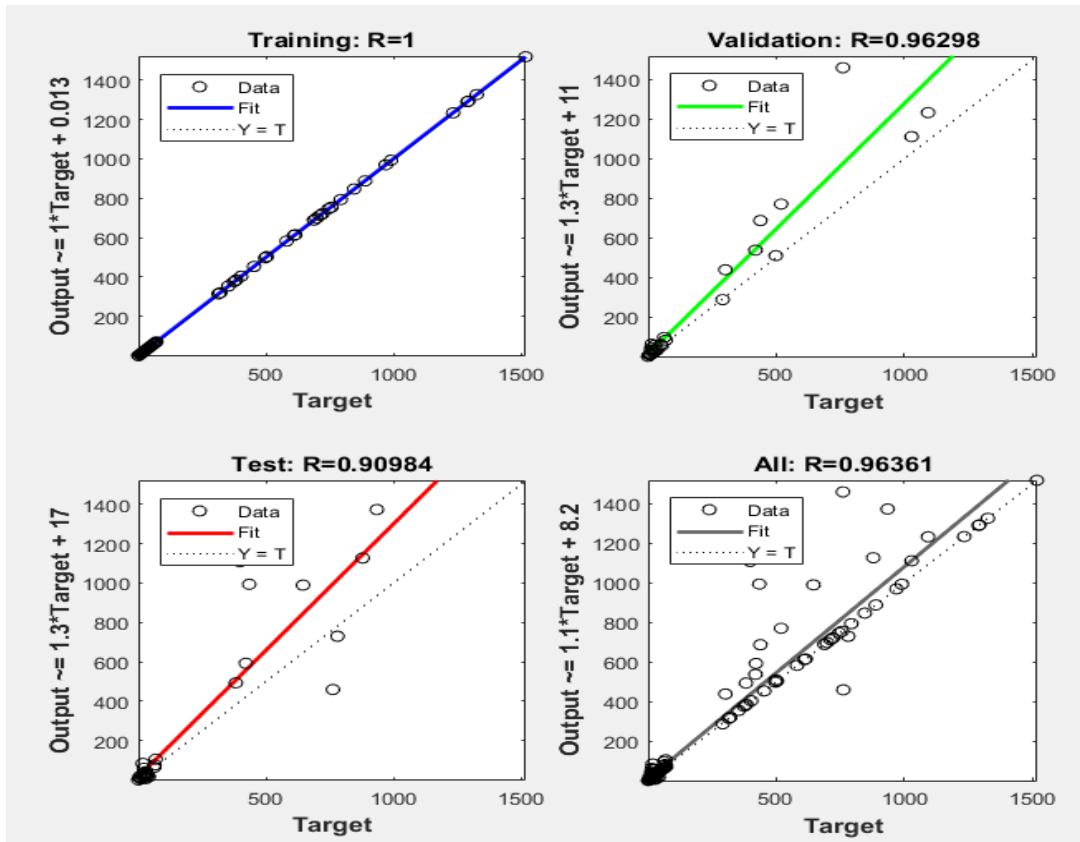


Fig. 2 ANN Output Graph for the Dataset

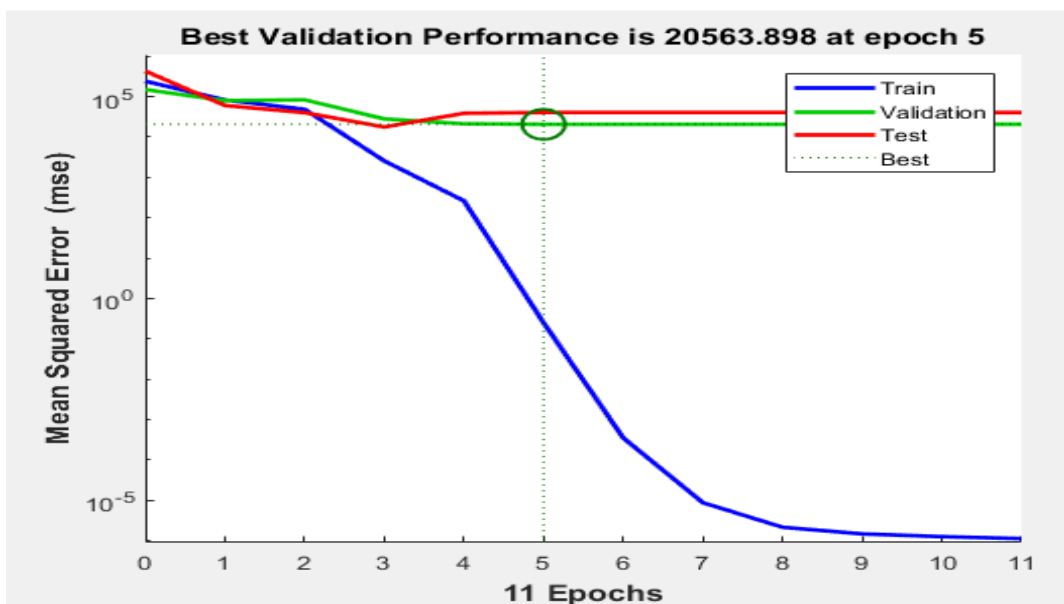


Fig. 3 ANN Training Graph for the Data Used

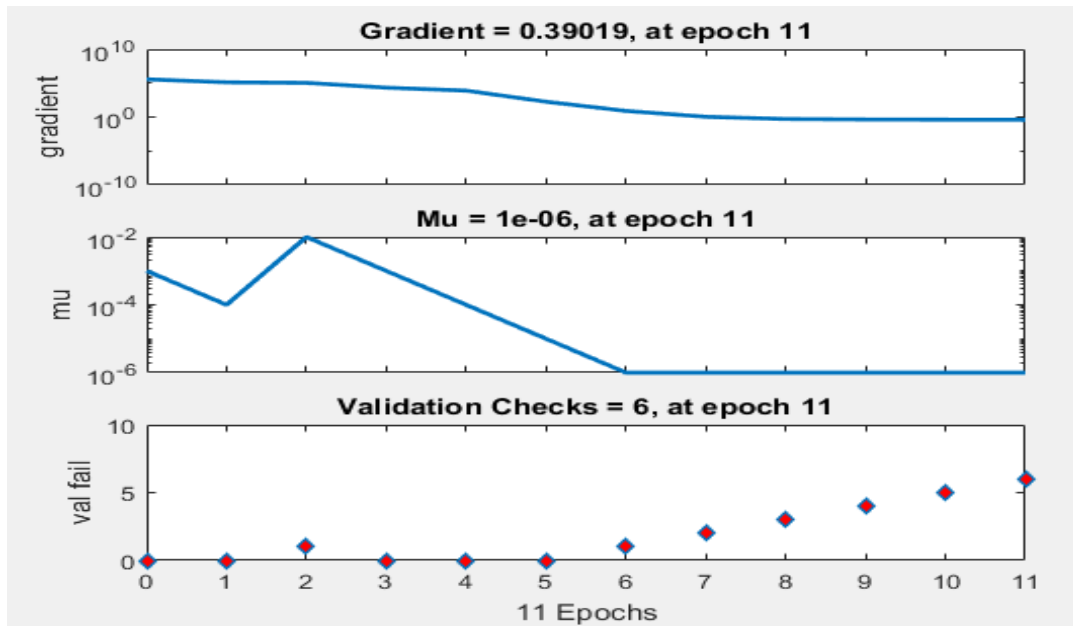


Fig. 4 The ANN Validation Checks, Mu and Gradient

3. Results and discussion

There were seventeen (17) specimens as indicated in Table 3. The first specimen contains no ceramic silicon carbide, whereas the remaining specimens were mixture of aluminium (97.5, 95.0, 92.5 and 90 wt %) and silicon carbide (2.5, 5.0, 7.5 and 10 wt %) as indicated in the first two columns. The third column showed variation of particle sizes of silicon carbide (3 μm, 9 μm, 29 μm and 45 μm). The seventeen specimens were characterized to obtain the eleven material properties for Al/SiCp composites listed in Table 4. These measured data were presented to ANN for training, validation and testing. ANN subsequently generated new set of predicted properties for all the seventeen specimens.

Figures 5-15 showed graphically the measured and ANN predicted properties for tensile extension (mm), hardness and electrical tests to obtain tensile extension (mm), load (N), modulus (N/mm²), yield strength (MPa), ultimate tensile strength (MPa), tenacity at fracture (gf/tex), time at fracture (s), hardness (HV), electrical conductivity (MΩ/m), electrical resistivity (μΩ-m) and tensile stress (MPa) respectively.

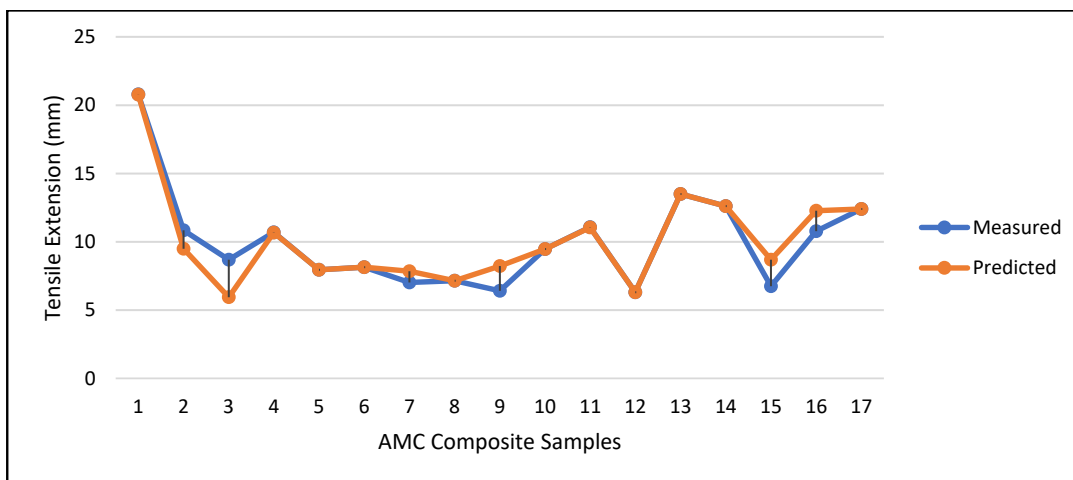


Fig. 5 Measured and predicted tensile extension properties of AMC Composites

It is observed that ANN predicted data is quite successful with perfect matches seen in ten (10) out of eleven (11) material properties. Aside resistivity, perfect predictions were seen in tensile extension (mm), load (N), modulus (N/mm²), yield strength (MPa), hardness (HV), ultimate tensile strength (MPa), tenacity at fracture (gf/tex), time at fracture (s), electrical conductivity(MΩ/m), and tensile stress (MPa) respectively.

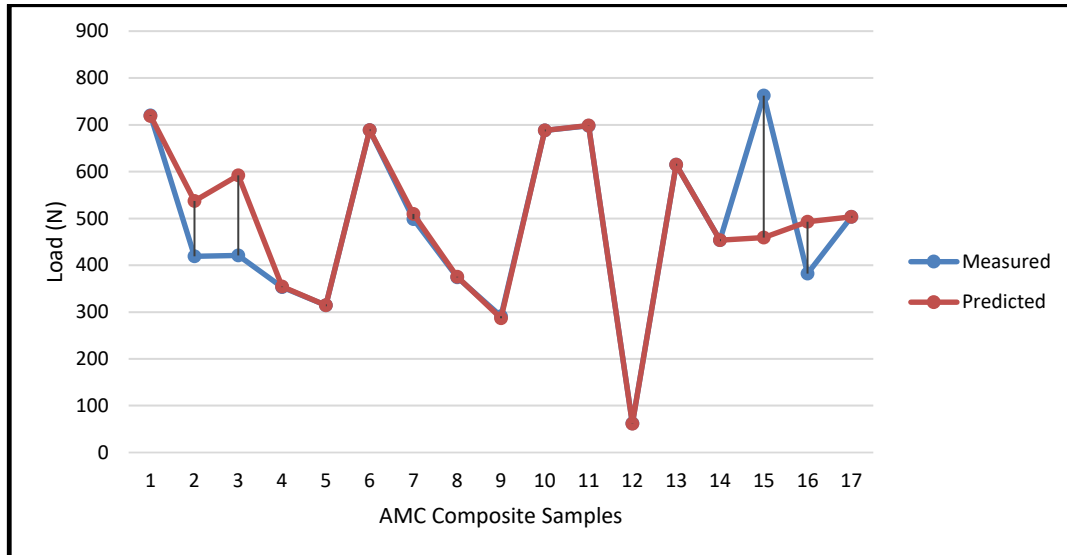


Fig. 6 Measured and predicted load of AMC Composites

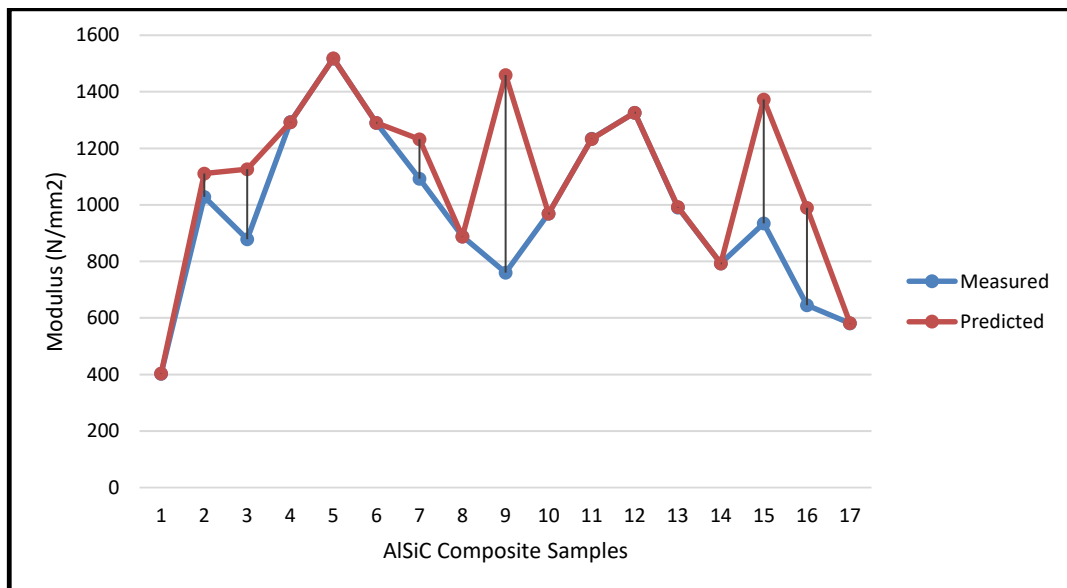


Fig. 7 Measured and predicted modulus of AMC Composites

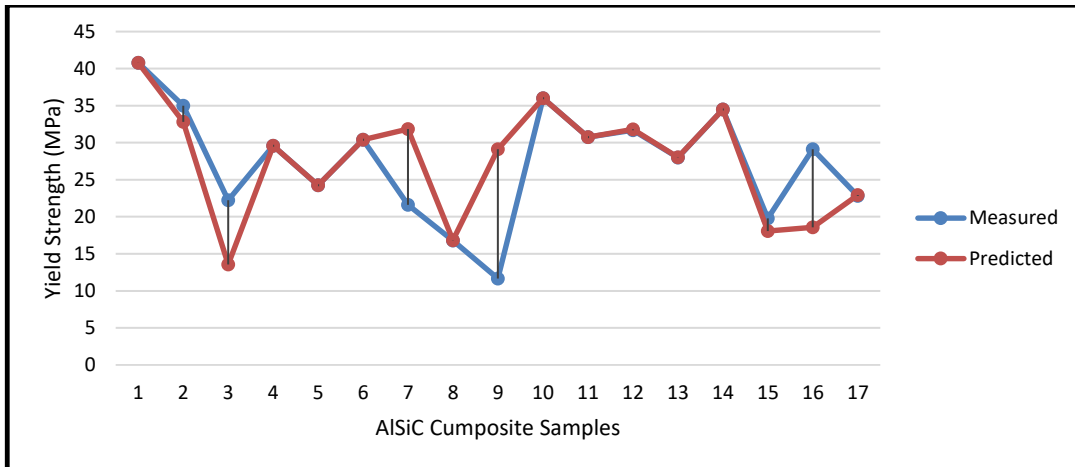


Fig. 8 Measured and predicted yield strength of AMC Composites

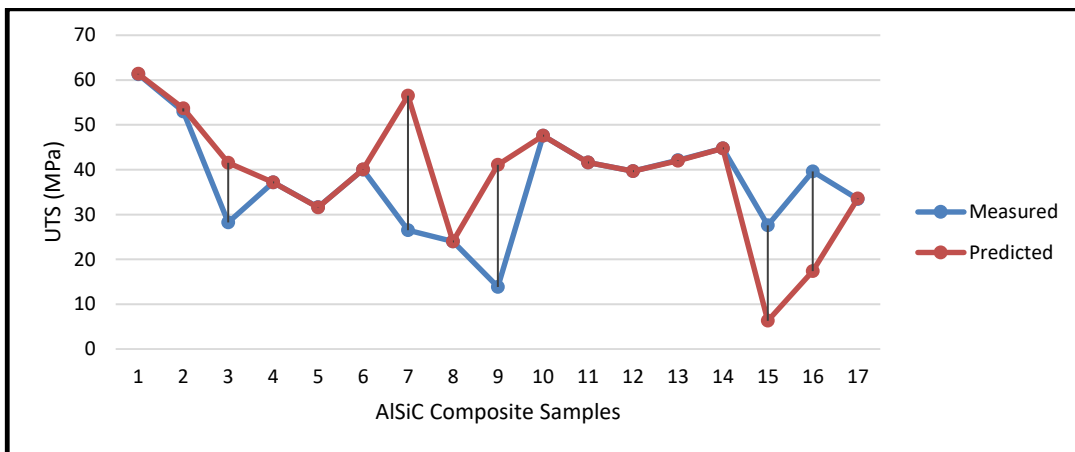


Fig. 9 Measured and predicted ultimate tensile strength of AMC Composites

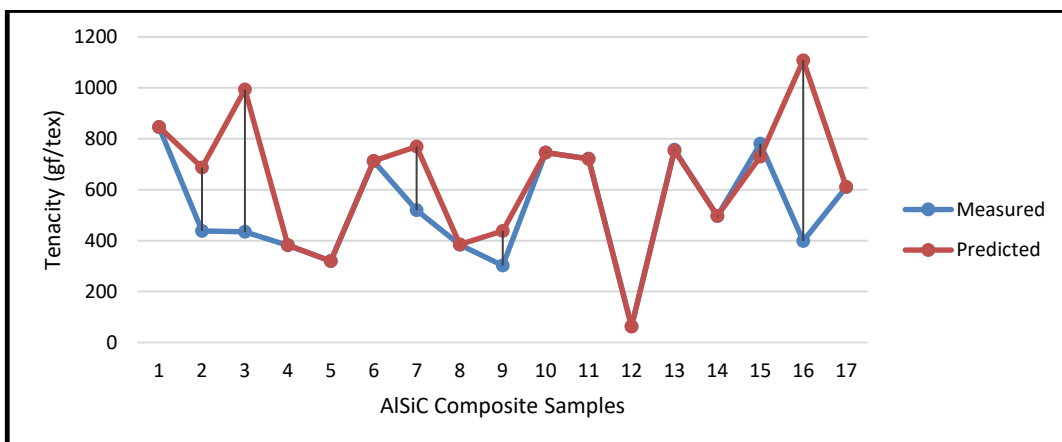


Fig. 10 Measured and predicted tenacity of AMC Composites

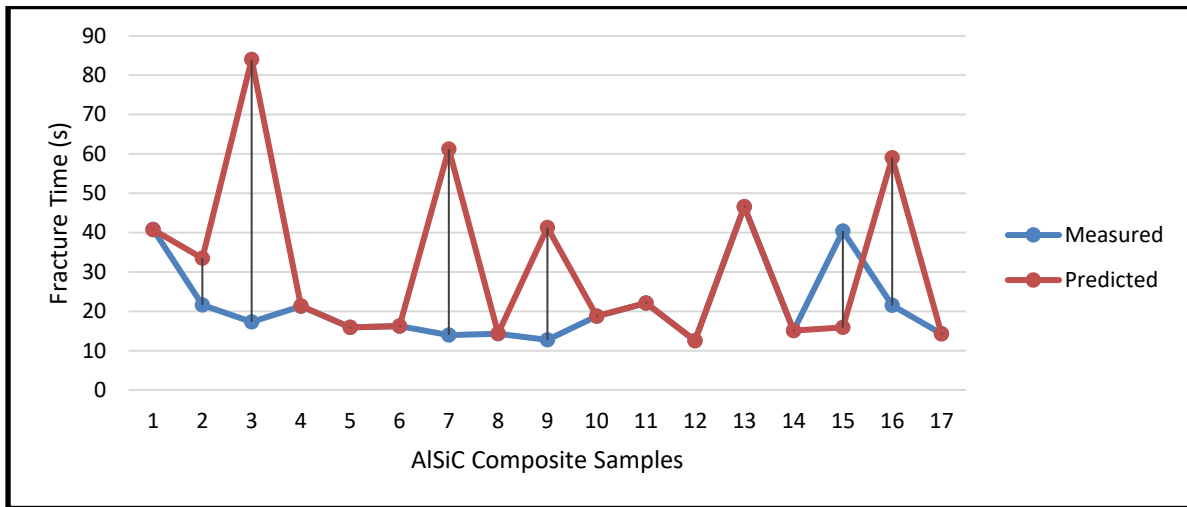


Fig. 11 Measured and predicted fracture time of AMC Composites

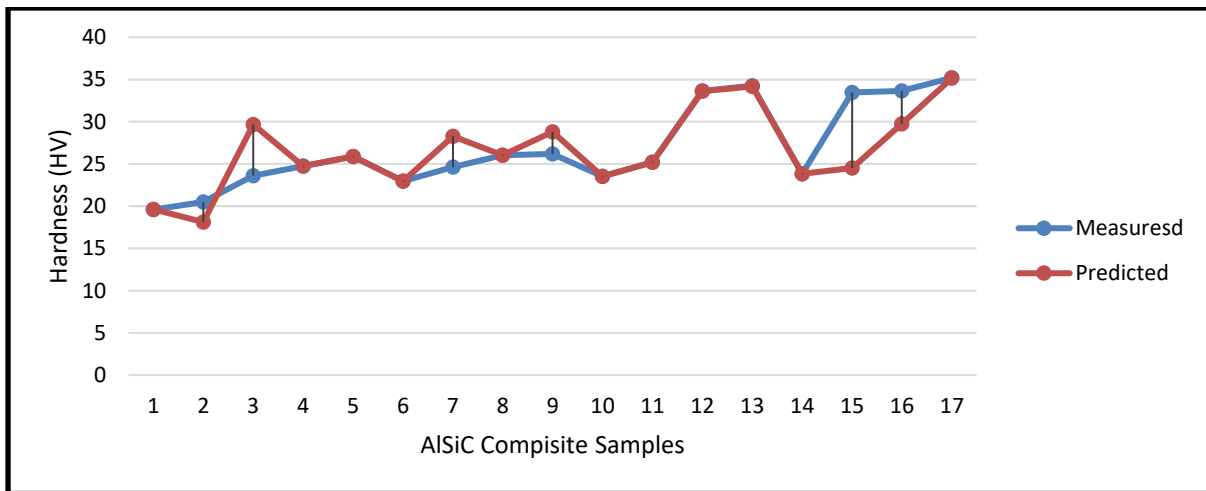


Fig. 12 Measured and predicted hardness of AMC Composites

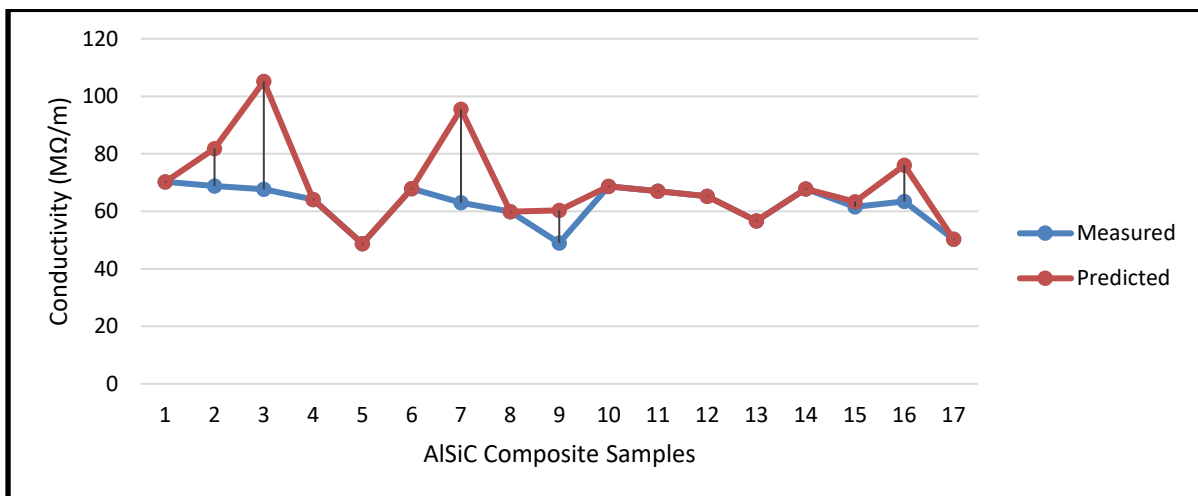


Fig. 13 Measured and predicted conductivity of AMC Composites

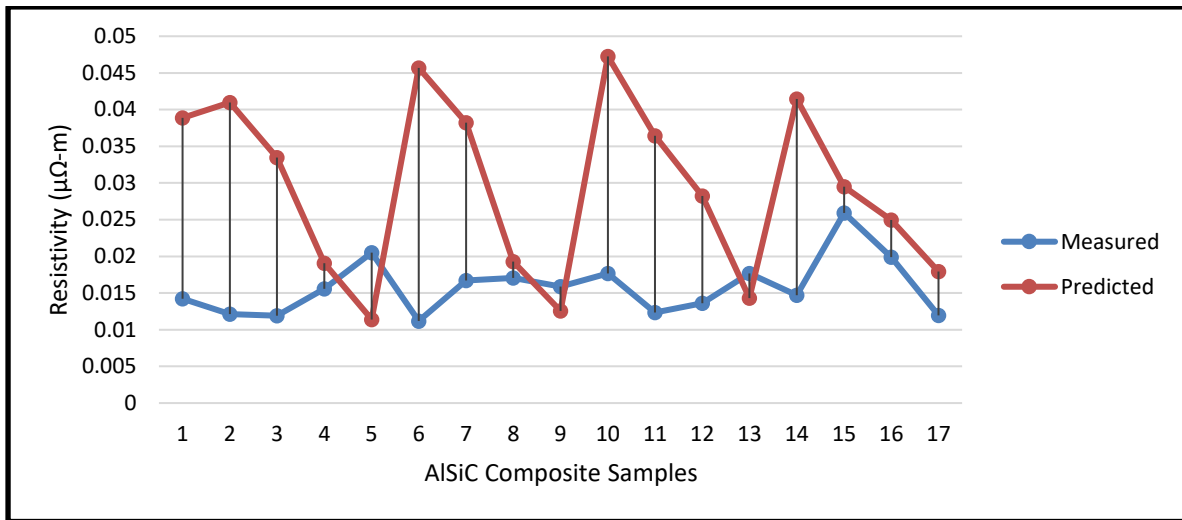


Fig. 14 Measured and predicted resistivity of AMC Composites

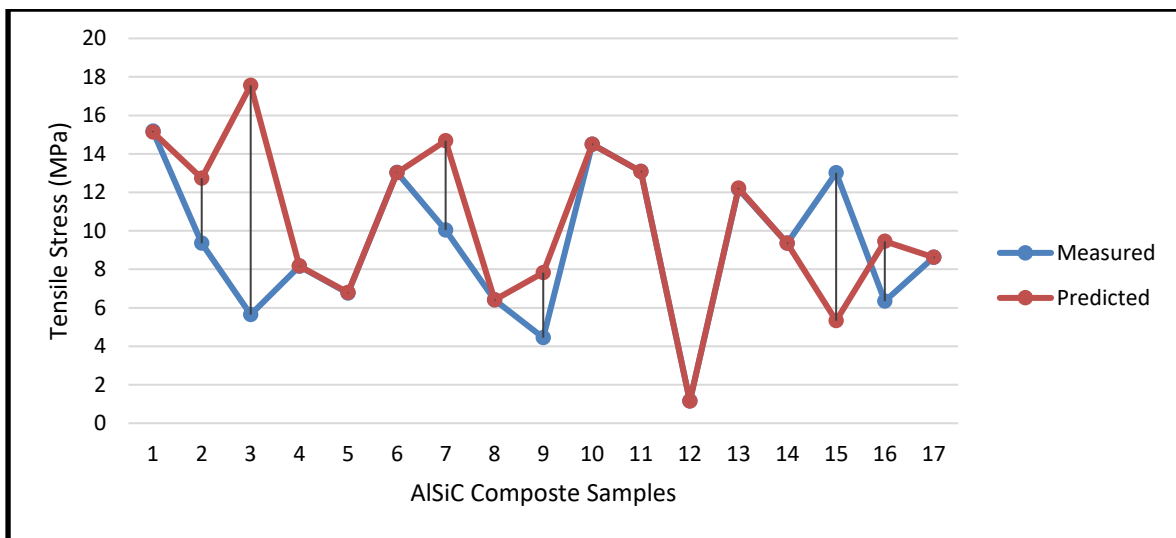


Fig. 15 Measured and predicted tensile stress of AMC Composites

4. Conclusions

In the present study, prediction of Al/SiCp composites with varied aluminium content, SiC content and silicon particle size was done. The following results were obtained:

- i. Artificial Neural Network (ANN) is a versatile and effective tool in forecasting composite properties. In an established processing route and constituent materials, the resultant composite material properties could be predicted by designers and process engineers, thereby saving cost in the process.
- ii. Forecasted tensile, electrical conductivity and hardness from ANN model were consistent and showed good agreement with measured results from the specimens.

Funding: The authors acknowledge Covenant University (CU) and Covenant University Centre for Research, Innovation and Discovery (CUCRID) Ota, Nigeria for the sponsorship and provision of research facilities for this work.

References

- [1] Davies G. *Materials for Automobile bodies*. Butterworth-Heinemann, Oxford, MA 01803, 2003, pp. 90.
- [2] Kok M, and Ozdin K. Wear resistance of aluminium alloy and its composites reinforced by Al₂O₃ particles. *Journal of Materials Processing Technology*, 2007, 183: 301–309.
- [3] Prabu S.B, Karunamoorthy L., Kathiresan S., and Mohan B. Influence of stirring speed and stirring time on distribution of particles in cast metal matrix composite. *Journal of Materials Processing Technology*, 2006, 171: 268–273.
- [4] Inegbenebor A.O., Bolu C.A., Babalola P.O., Inegbenebor A.I. and Fayomi O.S.I. Aluminum Silicon Carbide Particulate Metal Matrix Composite Development Via Stir Casting Processing. *Silicon*, 2016, DOI 10.1007/s12633-016-9451-7.
- [5] Inegbenebor A.O., Bolu C.A., Babalola P.O., Inegbenebor A.I. and Fayomi O.S.I. Influence of the Silicon Carbide Gritsize Particles on the Mechanical and Electrical Properties of Stir Casting Aluminum Matrix Composite Material. *Silicon*, 2015, DOI 10.1007/s12633-015-9305-8.
- [6] Babalola P.O, Bolu C.A, Inegbenebor A.O and Odunfa K.M. Development of Aluminium Matrix Composites: A review. *Online International Journal of Engineering and Technology Research*, ISSN 2346-7452; 2014, 2: 1-11.
- [7] Babalola P.O., Inegbenebor, A.O., Bolu, C.A., Inegbenebor, A.I. The Development of Molecular-Based Materials for Electrical and Electronic Applications. *JOM*, 2015, 67(4): 830-833.
- [8] Luan B.F., Hansen N., Godfrey A., Wu G.H., and Liu Q. High strength Al–Al₂O₃p composites: Optimization of extrusion parameters. *Materials and Design*, 2011, 32:3810–3817.
- [9] Singla M., Dwivedi D.D., Singh L., and Chawla V. Development of aluminium based silicon carbide particulate metal matrix composite. *Journal of Minerals & Materials Characterization & Engineering*, 2009, 8(6): 455-467.
- [10] Naher S., Brabazon D., and Looney L. Examination of the semi-solid stir casting method for producing Al-SiC metal matrix composites. *Materials Processing Research Centre, Dublin City University, Dublin 9, Ireland*, 2012.
- [11] Mohanavel V., Rajan K., Kumar S. S., Udishkumar S., Jayasekar C. Effect of silicon carbide reinforcement on mechanical and physical properties of aluminium matrix composites. *Materials Today: Proceedings*, 2018, 5:2938–2944.
- [12] Alaneme K. K., Bodunrin M.O., Awe A. A. Microstructure, mechanical and fracture properties of groundnut shell ash and silicon carbide dispersion strengthened aluminium matrix composites. *Journal of King Saud University – Engineering Sciences*, 2018, 30: 96-103.
- [13] Sulaiman S., Marjom Z., Ismail M.I.S, Ariffin M.K.A. and Ashrafi N. Effect of Modifier on Mechanical Properties of Aluminium Silicon Carbide (Al-SiC) Composites. *Procedia Engineering*, 2017, 184: 773 – 777.
- [14] Kavimani V., Prakash K.S. Tribological behaviour predictions of r-GO reinforced Mg composite using ANN coupled Taguchi approach. *Journal of Physics and Chemistry of Solids*, 2017, 110: 409–419.
- [15] Rashed F.S. and Mahmoud T.S. Prediction of wear behaviour of A356/SiCp MMCs using neural networks. *Tribology International*, 2009, 42: 642–648.
- [16] Ali S. Hammood, Haider Mahdi. Development Artificial Neural Network Model to Study the Influence of Oxidation Process and Zinc-Electroplating on Fatigue Life of Gray Cast Iron. *International Journal of Mechanical & Mechatronics Engineering, IJMME-IJENS*, 2012, 12(5):74-78.
- [17] Shandilya Pragya, Jain P.K., Jain N.K. RSM and ANN Modeling Approaches for Predicting Average Cutting Speed During WEDM of SiCp/6061 Al MMC. *Procedia Engineering*, 2013, 64: 767 – 774.